

**Loss-induced localization in a periodically driven nonlinear system**Liping Li,<sup>\*</sup> Xuehua Zhang, Lin Li, Qing He, Limin Zheng, Shiqiang Fu, and Bo Liu  
*College of Science, Zhongyuan University of Technology, Zhengzhou, 450007, People's Republic of China*

(Received 4 April 2019; published 9 September 2019)

We propose a scheme to study loss-induced localization in a nonlinear three-site system with a periodically driven field acting on the first site and a loss on the last site. We identify a significant feature; that is, system losses could be introduced to profoundly enhance localization. Our simulation results present two different types of localization: chaos-related localization and loss-induced localization, depending on their physical mechanisms. These findings may deepen our understanding about the relations among nonlinear effects, system loss, and external driving fields and offer a fascinating route towards the potential application for quantum control of tunneling dynamics.

DOI: [10.1103/PhysRevA.100.033808](https://doi.org/10.1103/PhysRevA.100.033808)**I. INTRODUCTION**

Quantum tunneling and localization are of fundamental importance and have been widely investigated [1–3]. Over the years, many localization schemes have been proposed, using various methods including atomic coherence, quantum interference effects [4–6], and external driven fields [7,8]. As is well known, manipulation of tunneling dynamics by control of external periodically driven field has become a hot topic because of its fascinating applications in quantum switching, motor, and transport [9–12]. Moreover, different types of localization are realized depending on their physical origins. For linear driven systems, coherent destruction of tunneling (CDT) [13–16] and dark-CDT [17] are two representative phenomena of localization. CDT occurs in a driven two-site system and its understanding is related to the degeneration of the quasienergy spectrum. Actually, Grossmann *et al.* found that, if the ratio of driving amplitude  $A$  to frequency  $\omega$  satisfied the zeroth-order Bessel function  $J_0(A/\omega) = 0$ , the driven site would be decoupled from the undriven site. Dark-CDT was first reported for a driven three-site system and is induced by localized dark Floquet states. For nonlinear driven systems, there always exists localization, such as Anderson localization [18,19] and chaos-related localization [20,21]. In one-dimensional waveguide arrays, Martin *et al.* [19] showed that Anderson localization could be realized by introducing off-diagonal disorder, and the strength of localization favored a higher level of disorder.

However, the above results are discussed in absence of system loss, which is unavoidable in realistic physical systems. Recently, lossy quantum systems have attracted increased attention and provide a way to study non-Hermitian Hamiltonians which obey parity-time symmetry in some specially designed systems [22]. Counterintuitively, it has been reported that system loss can lead to dramatic enhancement of localization [23]. Christodoulides *et al.* have reported a phenomenon of loss-induced localization in one-dimensional

PT-symmetric systems and have identified that the emergence of localized states are entirely due to the presence of loss [24]. Such interesting results have inspired a lot of work on lossy systems [25], and we are interested in what happens to loss-induced localization in a periodically driven system.

In this paper, we mainly discuss the influence of system loss on the dynamics of a driven three-site system, in which the combined effects of driving field, nonlinearity, and system loss are considered comprehensively. Our simulation results have shown that system losses can enhance localization significantly in some parameter regions. When the loss of a boundary site is very small, system dynamics in another boundary site are very sensitive to initial conditions and exhibit chaotic motion. The loss, in effect, playing a role of disorder, leads to chaos-related localization. With the increase of system loss, chaotic dynamics is destroyed eventually and the system evolves into the nonchaotic regime in which particles can be localized at the excitation lattice point only within a certain period of time. The transient nature of localization will be studied in detail and analyzed quantitatively. Surprisingly, when system losses are very large, almost complete loss-induced localization occurs since the lossy factor does not actually work, which means that the system is effectively lossless. Two completely different types of localization are then possible: chaos-related localization and loss-induced localization, depending on whether the dynamics are chaotic. Moreover, our results clearly reveal the relationship between loss-induced localization and chaos and offer a possibility to manipulate driving-controlled quantum states.

The structure of this paper is as follows: In Sec. II, two possible experimental models of a driven three-site quantum system are proposed. In Sec. III, we present a counterintuitive phenomenon of loss-induced localization based on discrete Schrödinger equations and further explore its possible physical origin. Moreover, two different types of localization, including chaotic localization and nonchaotic localization, are demonstrated and the profound influence of system loss on dynamics is studied. In Sec. IV, the dependence of loss-induced localization on driving parameters and nonlinearity

<sup>\*</sup>llp010910@163.com

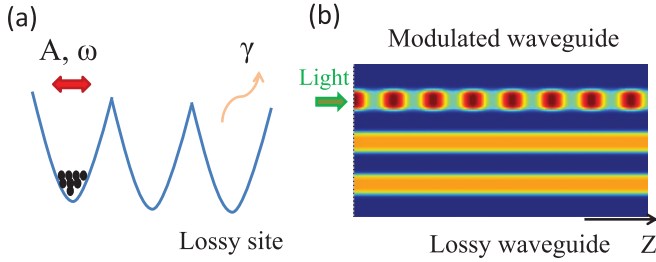


FIG. 1. (a) Schematic diagram for a driven three-site system. Here the left boundary site-1 is driven periodically with amplitude  $A$  and frequency  $\omega$ , and the right boundary site-3 has a loss coefficient  $\gamma$ . (b) Three-coupled waveguides with Kerr nonlinearity and light propagating in the  $z$  direction. The refractive index of upper waveguide-1 is modulated periodically and lower waveguide-3 is lossy.

is discussed in detail. In the last section, we draw a brief conclusion.

## II. MODELS

We propose two schemes in Fig. 1 to realize systems of dimension 3 with nonlinearity, periodic driving as well as loss. The models in Figs. 1(a) and 1(b) are defined separately as model A and model B. Model A consists of three coupled sites in a linear arrangement with a periodic driving field acting on the left boundary site (site 1) and loss only at the right boundary site (site 3), as shown in Fig. 1(a). Model A has been used theoretically by many researchers to study the coherent control of tunneling dynamics [26,27]. Through launching a Bose-Einstein condensate [28,29] in a driven three-linear-coupled potential well, such a model could be experimentally implemented by means of equipment which permits a tunneling contact between adjacent sites. The interatomic interaction could be adjusted by Feshbach resonances [30] and may lead to a nonlinear term in the coupled dynamic equations. The system dynamics in Model A could be evaluated from the probability amplitudes of the atomic population distribution at different sites.

Moreover, since the propagation of light in coupled optical waveguides may resemble the motion of atoms in coupled quantum potentials, our system could also be realized by designing three coupled optical waveguides with Kerr nonlinearity [31], as shown in Fig. 1(b), in which waveguide-1 is driven periodically by modulating the refractive index along the  $z$  direction and waveguide-3 is lossy. By mapping the time evolution of the atomic dynamics into the spatial propagation of light, the coupled waveguide system provides an alternative platform to realize optical analogies of quantum tunneling dynamics. Experimentally, the technology of fs laser written waveguide arrays permits our specific setting of the nonlinear guiding properties of the waveguides [32,33]. Longhi *et al.* [34,35] have suggested several methods to fabricate photonic lattices with a shaken partial lattice while keeping the rest fixed such as the boundary waveguide can have a different refractive index profile compared with the remaining waveguides. The system dynamics in Model B could be characterized by the evolution of the probability distribution of light intensity in different waveguides.

## III. LOSS-INDUCED LOCALIZATION IN THE DRIVEN NONLINEAR SYSTEM

### A. Chaos-related localization and loss-induced localization

In our analysis, we investigate dynamics according to Model A; similar behavior may appear in Model B as well. Here, we assume that a Bose-Einstein condensate with  $N$  identical bosons is launched into lossless site-1 initially and only occupies three quantum states. In the mean-field approximation and with the interaction between atoms considered, the nonlinear three-mode system can be described by discrete Schrödinger equations [36–38],

$$\begin{aligned} i\frac{da_1(t)}{dt} &= A \cos(\omega t)a_1(t) + \Omega a_2(t) + K|a_1(t)|^2 a_1(t), \\ i\frac{da_2(t)}{dt} &= \Omega(a_1(t) + a_3(t)) + K|a_2(t)|^2 a_2(t), \\ i\frac{da_3(t)}{dt} &= -i\gamma a_3(t) + \Omega a_2(t) + K|a_3(t)|^2 a_3(t), \end{aligned} \quad (1)$$

where  $\Omega$  is the coupling constant of nearest-neighbor sites and  $\gamma$  is the loss rate in site-3. Here, a cosine driving field acts on site-1 with driving amplitude  $A$  and driving frequency  $\omega$  and  $K$  is the nonlinearity between atoms. All the parameters are normalized such that  $A$ ,  $\omega$ ,  $\Omega$ , and  $K$  are in units of a reference frequency  $\omega_0$  on the order of  $10^2 \text{ s}^{-1}$  [39], and time  $t$  is normalized in units of  $\omega_0^{-1}$ . Variables  $a_1(t)$ ,  $a_2(t)$ ,  $a_3(t)$  are proportional to the macroscopic amplitudes of the atomic density in site-1, site-2, and site-3, respectively, and  $|a_j(t)|^2$  ( $j = 1, 2, 3$ ) denote the number of atoms in the  $j$ th potential well. When the number  $N$  of bosons is very large, it is appropriate to make the following substitutions:

$$\begin{aligned} \tilde{a}_1 &= a_1(t)/\sqrt{P(0)}, & \tilde{a}_2 &= a_2(t)/\sqrt{P(0)}, \\ \tilde{a}_3 &= a_3(t)/\sqrt{P(0)}. \end{aligned} \quad (2)$$

Here  $P(0) = |a_1(0)|^2 + |a_2(0)|^2 + |a_3(0)|^2$  is proportional to the total initial number  $N$  of bosons in the condensate. However,  $P(t) = |a_1(t)|^2 + |a_2(t)|^2 + |a_3(t)|^2$ , which represents total atoms at time  $t$ , is not a conserved quantity due to the loss  $\gamma$ . We would like to emphasize that what is essential is the ratios between these parameters, not their absolute values. To investigate tunneling dynamics, we introduce probabilities  $P_j(t)$  as normalized ratios,

$$P_j(t) = |a_j(t)|^2/P(0) = |\tilde{a}_j|^2. \quad (3)$$

Then the tunneling dynamics can be explored by the evolution of  $P_j(t)$  versus time  $t$  in different sites. For example,  $P_1(t) > 0.5$  means that more than 50% of all particles are situated in the first well and the dynamics in this case could be called localization. Moreover, the minimum value of  $P_1(t)$  [viz.,  $\min(P_1)$ ] is used in this paper to measure the degree of localization. When  $\min(P_1)$  equals about zero, the atoms can tunnel into other sites, while  $\min(P_1) > 0.5$  means localization in site-1. Apparently, a higher value of  $\min(P_1)$  means a higher degree of localization.

To facilitate our discussion, the complex numbers  $a_j(t)$  are replaced by  $\tilde{a}_j$  and further rewritten by using real numbers (viz.,  $\tilde{a}_j = b_j + ic_j$ ), where  $b_j$  and  $c_j$  are real numbers. Then,

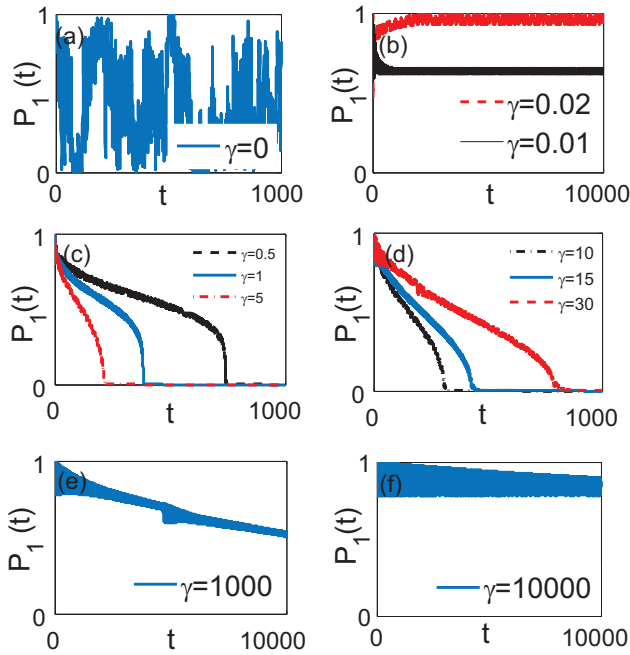


FIG. 2. Probability  $P_1(t) = |a_1|^2$  at site 1 versus time  $t$  under different cases of (a)  $\gamma = 0$ ; (b)  $\gamma = 0.01, 0.02$ ; (c)  $\gamma = 0.5, 1, 5$ ; (d)  $\gamma = 10, 15, 30$ ; (e)  $\gamma = 1000$ , and (f)  $\gamma = 10000$  separately. Other parameters are  $A = 16$ ,  $\omega = 10$ ,  $\Omega = 1$ , and  $U = 8$ .

the coupled equations Eq. (1) can be rewritten as

$$\begin{aligned}
 \frac{db_1}{dt} &= A \cos(\omega t)c_1 + \Omega c_2 + U|b_1|^2c_1 + U|c_1|^2c_1, \\
 \frac{dc_1}{dt} &= -A \cos(\omega t)b_1 - \Omega b_2 - U|b_1|^2b_1 - U|c_1|^2b_1, \\
 \frac{db_2}{dt} &= \Omega c_1 + \Omega c_3 + U|b_2|^2c_2 + U|c_2|^2c_2, \\
 \frac{dc_2}{dt} &= -\Omega b_1 - \Omega b_3 - U|b_2|^2b_2 - U|c_2|^2b_2, \\
 \frac{db_3}{dt} &= -\gamma b_3 + \Omega c_2 + U|b_3|^2c_3 + U|c_3|^2c_3, \\
 \frac{dc_3}{dt} &= -\gamma c_3 - \Omega b_2 - U|b_3|^2b_3 - U|c_3|^2b_3.
 \end{aligned} \quad (4)$$

Here the nonlinear coefficient  $U = KP(0)$  has been studied by Anker *et al.* [28] and its value can be manipulated through controlling the number of atoms. Unlike Eq. (1), all variables in Eq. (4) are real and the relative population probability at site-1 can be described by  $P_1(t) = |\tilde{a}_1|^2 = |b_1|^2 + |c_1|^2$ .

Now, we attempt to thoroughly investigate the profound influence of system losses on the dynamics. By integrating the coupled differential equations (4), under the initial conditions of  $b_1(0) = 1$ ,  $c_1(0) = 0$ ,  $b_2(0) = 0$ ,  $c_2(0) = 0$ ,  $b_3(0) = 0$ ,  $c_3(0) = 0$ , the evolution of probability  $P_1(t)$  versus time  $t$  with different values of  $\gamma$  and different integration times is shown in Figs. 2(a)–2(f). Other system parameters are chosen to be  $A = 16$ ,  $\omega = 10$ ,  $\Omega = 1$ , and  $U = 8$ . The driving amplitude and frequency are carefully chosen away from the point  $A/\omega = 2.4$ , which is a root of  $J_0(A/\omega) = 0$ , to ensure that localization here has no direct relationship to

CDT phenomenon [13]. Our simulation results reveal that, if  $\gamma = 0$  [see Fig. 2(a)], the atoms can tunnel back and forth among the three sites. However, in the case of  $\gamma = 0.01$ , as shown in Fig. 2(b), the result clearly suggests significantly improved localization and the degree of localization could be enhanced further when  $\gamma = 0.02$ . More simulation proves that localization keeps good stability even though total evolution time is extended to five orders of magnitude (not listed here).

When  $\gamma$  is more than 0.1, unexpectedly, localization cannot continue anymore and localization can mostly be maintained for a while, followed by tunneling dynamics. The duration of localization exhibits a trend of fall-rise with the increase of loss  $\gamma$ , and the turning point is about  $\gamma = 5$ . The cases of  $\gamma = 0.5, 1, 5$  are listed in Fig. 2(c) from top to bottom and show that a larger loss  $\gamma$  may lead to a shorter duration of localization. On the contrary, the duration of localization increases gradually through comparing the three cases of  $\gamma = 10, 15, 30$  as shown in Fig. 2(d). It is remarkable that the loss  $\gamma$  in our proposal can induce localization in a certain period of time; however, localization in Figs. 2(c) and 2(d), in fact, is not truly localization because the leakage may occur after a period of evolution time. The transient nature of the localization process in Figs. 2(c) and 2(d) is real since all densities are zero in the limit  $t \rightarrow \infty$ . Further calculation shows that  $\frac{dP(t)}{dt} = -2\gamma|a_3|^2$ . Thus the total number of atoms is a monotonically decreasing function, which is quite natural since the losses are not compensated by any gain. As a result, any localization in this lossy system would be only a transient process and we highlight the importance of integration times in observing localization.

Surprisingly, when  $\gamma$  increases even larger, such as  $\gamma = 1000$  [see Fig. 2(e)], the probability distribution of  $P_1(t)$  remains greater than 0.5 even if the total time  $t$  is extended by four orders of magnitude. Then, when  $\gamma = 10000$ , as shown in Fig. 2(f), greatly enhanced localization is observed again. The quantitative explanation for this phenomenon is quite clear: when the losses are very large, the number of atoms in the lossy site is always close to zero. Since the sites are coupled linearly through coefficient  $\Omega$ , atoms from the central site do not tunnel to the lossy site, so the lossy site is not excited and actually remains empty for all times, i.e., the lossy term  $-i\gamma a_3(t)$  in Eq. (1) does not actually work, which means that the system is effectively lossless. This behavior resembles the macroscopic Zeno effect for Bose-Einstein condensates, which consists in a decay of the atomic flux under the increase of the spatially localized dissipation [40]. However, because integration time cannot be infinite, localization, in fact, is hardly to be defined precisely. So we should emphasize that the concept of localization will be used in this paper if atoms can be localized during all the evolution. In a nutshell, it is clear that a slight change of system loss may lead to a large change of dynamics and a larger loss in such a driven system will not always mean a larger decay.

To understand its physical origin, we note that the system dynamics is irregular when  $\gamma = 0$ . Generally, the presence of the periodically driven field and nonlinearity may lead to chaos, so the physics of localization may be closely related to the chaotic behavior. Then, in order to verify our hypothesis and further study the sensitivity of system dynamics to initial conditions, a small quantity  $\vec{\epsilon} = (\epsilon_{b_1}, \epsilon_{c_1}, \epsilon_{b_2}, \epsilon_{c_2}, \epsilon_{b_3}, \epsilon_{c_3})$  is

defined to describe the adjacent trajectories of two nearby points moving forward in phase space. The effect of small deviations of initial conditions on system dynamics will provide us some evidence of chaos. By linearizing Eq. (4), the evolution equations about  $\bar{\varepsilon}$  are yielded,

$$\begin{aligned} \frac{d\varepsilon_{b_1}}{dt} &= A \cos(\omega t)\varepsilon_{c_1} + \Omega\varepsilon_{c_2} + U|b_1|^2\varepsilon_{c_1} \\ &\quad + 3U|c_1|^2\varepsilon_{c_1} + 2Ub_1c_1\varepsilon_{b_1}, \\ \frac{d\varepsilon_{c_1}}{dt} &= -A \cos(\omega t)\varepsilon_{b_1} - \Omega\varepsilon_{b_2} - U|c_1|^2\varepsilon_{b_1} \\ &\quad - 3U|b_1|^2\varepsilon_{b_1} - 2Ub_1c_1\varepsilon_{c_1}, \\ \frac{d\varepsilon_{b_2}}{dt} &= \Omega\varepsilon_{c_1} + \Omega\varepsilon_{c_3} + U|b_2|^2\varepsilon_{c_2} + 3U|c_2|^2\varepsilon_{c_2} + 2Ub_2c_2\varepsilon_{b_2}, \\ \frac{d\varepsilon_{c_2}}{dt} &= -\Omega\varepsilon_{b_1} - \Omega\varepsilon_{b_3} - U|c_2|^2\varepsilon_{b_2} \\ &\quad - 3U|b_2|^2\varepsilon_{b_2} - 2Ub_2c_2\varepsilon_{c_2}, \\ \frac{d\varepsilon_{b_3}}{dt} &= -\gamma\varepsilon_{b_3} + \Omega\varepsilon_{c_2} + U|b_3|^2\varepsilon_{c_3} \\ &\quad + 3U|c_3|^2\varepsilon_{c_3} + 2Ub_3c_3\varepsilon_{b_3}, \\ \frac{d\varepsilon_{c_3}}{dt} &= -\gamma\varepsilon_{c_3} - \Omega\varepsilon_{b_2} - U|c_3|^2\varepsilon_{b_3} \\ &\quad - 3U|b_3|^2\varepsilon_{b_3} - 2Ub_3c_3\varepsilon_{c_3}. \end{aligned} \quad (5)$$

The dynamics of nearby points ( $P_1 + \varepsilon_{P_1}$ ) of  $P_1$  are accounted to characterize the deviation of population distribution. The corresponding trajectory curve of  $\ln(\varepsilon_{P_1})$  versus time  $t$  is usually used to describe chaotic dynamics and a rising trend in general implies the existence of chaos. Choosing initial values  $\bar{\varepsilon} = (10^{-20}, 10^{-20}, 10^{-20}, 10^{-20}, 10^{-20}, 10^{-20})$ ,  $\ln(\varepsilon_{P_1})$  versus time  $t$  is plotted in Figs. 3(a)–3(d) with four different values for  $\gamma$ . When  $\gamma = 0$ , the curve in Fig. 3(a) keeps rising for 600 time units and no saturation is observed. When  $\gamma = 0.01$ , as shown in Fig. 3(b), the saturation occurs at about 150 time units, while it just needs 30 time units to reach saturation when  $\gamma = 0.02$  [see Fig. 3(c)]. More simulation results reveal that, when  $\gamma > 0.1$ , chaos is destroyed and the trajectory curves are almost flat such as when  $\gamma = 0.2$  in Fig. 3(d). Comparing with the results in Fig. 2, we can conclude briefly that, (i) when loss is very small,  $\gamma$ , in effect, plays the role of disorder, which means that for larger  $\gamma$  the saturation occurs quicker, while for smaller  $\gamma$  saturation might occur for high values of  $t$ . Thus, localization in Fig. 2(b) is chaos-related localization. (ii) With the increase of  $\gamma$ , the chaotic dynamics will quickly be destroyed, leading to localization in a certain evolution time, and the population properties will decline to zero after a period of time, which may due to impedance matching between lattice points. (iii) When  $\gamma$  becomes very large, the lossy site is not excited and almost complete localization will be observed again.

These results reveal that loss can be generally introduced to induce localization in a certain evolution time; however, highly enhanced localization can be observed just when  $\gamma$  is very small or very large. In addition, two types of localization: chaos-related localization and loss-induced localization are observed depending on whether localization is chaotic.

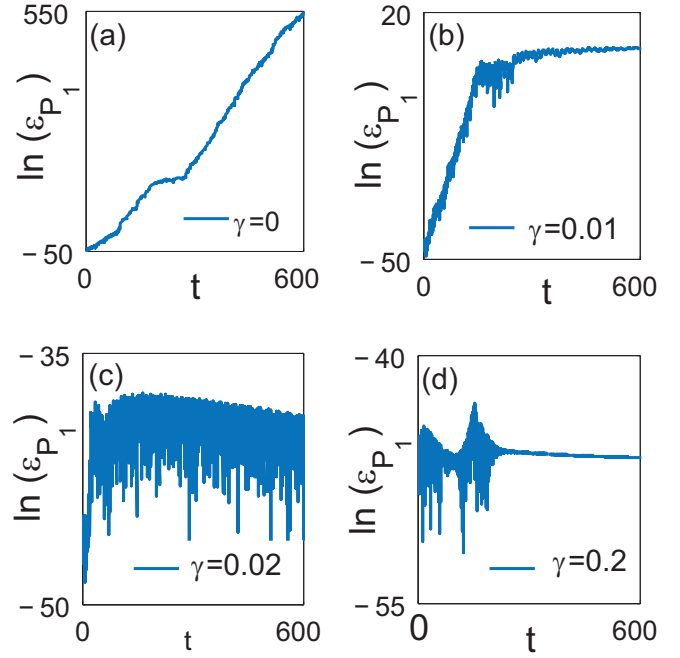


FIG. 3. Trajectory curves of  $\ln(\varepsilon_{P_1})$  versus time  $t$  with 600 time units in the cases of (a)  $\gamma = 0$ ; (b)  $\gamma = 0.01$ ; (c)  $\gamma = 0.02$ ; and (d)  $\gamma = 0.2$  separately. Other parameters are  $A = 16$ ,  $\omega = 10$ ,  $\Omega = 1$ , and  $U = 8$ .

### B. Loss-induced localization and its physical origin

To make a more intensive study of the influence of  $\gamma$  on localization, the minimum value of  $P_1(t)$  in a period of evolution time with the increase of  $\gamma$  is plotted in Fig. 4(a). To make a comparison between different evolution time, the results with 100 and 1000 time units are both studied. Other parameters are  $A = 16$ ,  $\omega = 10$ ,  $U = 8$  and all atoms have been assumed to be launched into the first well initially. When  $\gamma$  varies from 0 to 0.1 and the total evolution time is 100 time units, multiple transitions between tunneling and localization are observed. Localization in the parameter region of  $0 < \gamma < 0.1$  is not stable and a slight change of system loss may induce the disappearance of localization. On the other hand, when  $\gamma$  is more than 0.1, localization seems insensitive to parameter loss and atoms may always be localized at site-1 at all evolution times. Then, when the total evolution time is extended to 1000 time units, the simulation result [see dashed line in Fig. 4(a)] shows an obvious decline when  $\gamma$  is more than 0.15 and indicates a decrease of the degree of localization with an extended time.

The evolution properties are further studied within a wider parameter range of loss  $\gamma$  in Fig. 4(b). The upper black line corresponds to a shorter evolution time (100 time units), while the lower red dashed line corresponds to a longer evolution time (1000 time units). When  $\gamma$  varies from 0 to 100, both curves in Fig. 4(b) show a trend of fall-rise and the result may provide a way to enhance the degree of localization in site-1 through enhancing the losses in site-3. In particular, as the loss becomes even larger, the two curves get closer and the influence of evolution time becomes weaker. This counterintuitive phenomenon agrees well with the result in

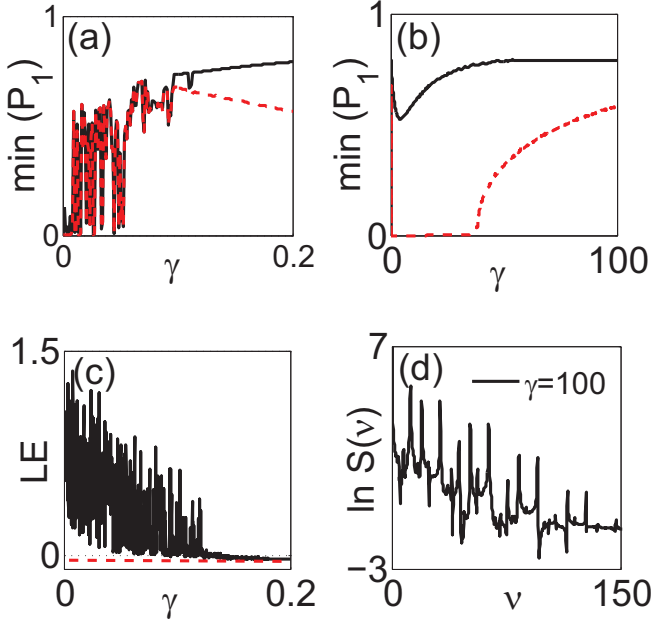


FIG. 4. Evolution of  $\min(P_1)$  as a function of loss  $\gamma$  when (a)  $\gamma$  varies from 0 to 0.2 and (b)  $\gamma$  varies from 0 to 100. Red dashed lines represent the cases when total evolution time is extended to 1000 time units. (c) Lyapunov exponent versus loss  $\gamma$  within the parameter range between 0 and 0.2. The horizontal dashed line in panel (b) labels the positions of  $\alpha = 0$ . (d)  $\ln S(\nu)$  versus frequency  $\nu$  when  $\gamma = 100$ . Other parameters are  $A = 16$ ,  $\omega = 10$ ,  $\Omega = 1$ , and  $U = 8$ .

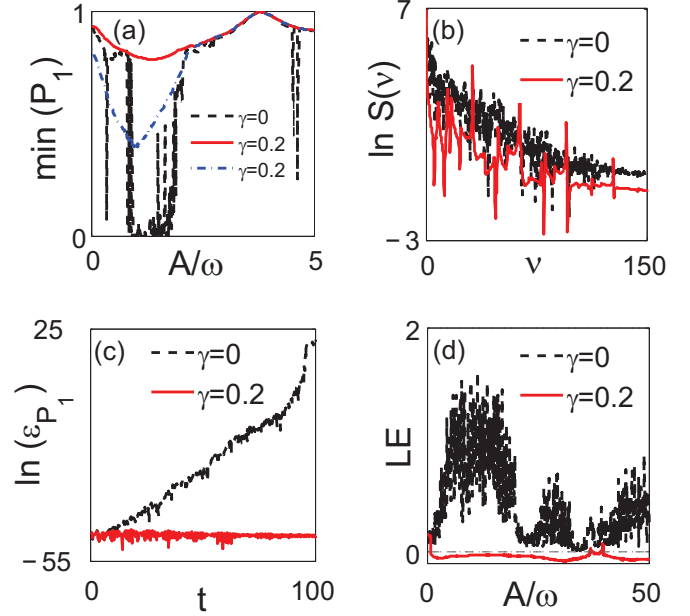


FIG. 5. A comparison of atomic dynamics between  $\gamma = 0$  and  $\gamma = 0.2$ . (a) The minimum value of  $P_1(t)$  as a function of  $A/\omega$  with two different integration times: 100 time units (black dashed line and red solid line) and 1000 time units (blue dash-dotted line). (b) Spectrum  $S(\nu)$  of  $P_1(t)$  versus frequency  $\nu$ . (c) The corresponding trajectory curve of  $\ln(\varepsilon_{P_1})$  versus time  $t$ . (d) Lyapunov exponent ( $LE$ ) as a function of  $A/\omega$ . Other parameters are  $A = 16$ ,  $\omega = 10$ ,  $\Omega = 1$ , and  $U = 8$ .

Ref. [23], and we further prove that localization could also be realized in a lossy nonlinear periodically driven system.

To find out physical origins, relationship between dynamics and chaos is studied. As shown in Fig. 4(c), the curve of the Lyapunov exponent ( $LE$ ), which is the logarithmic slope of the curve  $\ln(\varepsilon_{P_1})$  versus time  $t$ , shows that the  $LE$  continues to decrease until  $\alpha \leq 0$  with the increase of losses. The horizontal dashed line in Fig. 5(c) labels the position of  $\alpha = 0$ . Specifically, when  $\gamma$  is much smaller than 0.1, the Lyapunov exponent is larger than zero and the dynamic is chaotic. Eventually, when  $\gamma$  is more than 0.15, the exponent may decrease less than zero and chaos disappears completely. So, it is the chaos that determines the type of localization, and such results are consistent with those in Figs. 2 and 3. Besides, to further verify whether there is an existence of chaotic phenomenon when  $\gamma = 100$ , the spectrum  $S(\nu)$  attained by using fast Fourier transform of  $P_1 = |b_1|^2 + |c_1|^2$  is studied to analyze the spectrum information in the function of  $P_1(t)$ . Here, to avoid confusion with the driving frequency  $\omega$ , the frequency information is denoted by  $\nu$  and usually the spectrum of chaos is successive.  $\ln S(\nu)$  versus frequency  $\nu$  is shown in Fig. 4(d), and the discrete spectrum demonstrates that loss-induced localization when  $\gamma = 100$  is not chaotic.

Briefly, system loss  $\gamma$  has a profound influence on the system dynamics. When  $\gamma$  is smaller than 0.1, the dynamics are chaotic and exhibit multiple transitions between chaos-related localization and tunneling. However, larger system loss may destroy the chaotic dynamics and finally lead to loss-induced localization.

## IV. DISCUSSION

### A. Dependence of localization on driving parameters

In the later sections, we just consider the cases with weak loss and short evolution time. The initial conditions are the same as in Fig. 2. First, we discuss the dependence of localization on driving parameters. The evolution of  $\min(P_1)$  as a function of  $A/\omega$  with 100 time units is plotted in Fig. 5(a) with a nonlinearity  $U = 8$ . In the case of  $\gamma = 0$  (black dashed line),  $\min(P_1)$  decreases to zero, followed by a variation of between 0 and 0.8, which denotes multiple transitions between tunneling and localization and ends up with a plateau representing a stable localization. It is clear from the upper line (red solid line) in Fig. 5(a) that, for the case of  $\gamma = 0.2$ ,  $\min(P_1)$  is always more than 0.5. Consequently, transition from localization to delocalization disappears and tunneling is greatly suppressed. In particular, we emphasize that loss-induced localization when  $\gamma = 0.2$  (the red solid line) also corresponds to some intermediate stage of the transient process, which is clear from Figs. 2(c) and 2(d), and changing the integration time from 100 time units to another value can affect the obtained pictures. The blue dash-dotted line in Fig. 5(a) shows the result with 1000 time units and obviously the degree of localization decreases similar as in Fig. 4(a). Briefly, we find out that system losses can dramatically enhance the localization within a wide range of driving parameter windows when  $A/\omega$  ranges from 1 to 2. Our results clearly demonstrate that loss could be introduced to induce localization in a nonlinear periodically driven system within a

certain parameter range, which is known as the phenomenon of loss-induced localization.

To understand the underlying physics of localization, fixing the driving amplitude  $A = 16$ , frequency  $\omega = 10$ , and nonlinearity  $U = 8$ , the spectrum information  $S(\nu)$  for the cases of  $\gamma = 0$  and  $0.2$  is shown in Fig. 5(b). Clearly, when  $\gamma = 0$ , the successive spectrum suggests chaotic dynamics. After adding system loss, the discrete spectrum when  $\gamma = 0.2$  generally represents nonchaotic motion. The results indicate that loss-induced localization in our proposal may be nonchaotic.

To get more evidence of chaos, we plot the corresponding trajectory curve of  $\ln(\varepsilon_{P_1})$  versus time  $t$  in Fig. 5(c) under the conditions of  $\gamma = 0$  and  $0.2$  separately. The rising curve when  $\gamma = 0$  may imply that, with increasing time, an incredibly tiny variation of initial conditions may lead to an exponential increase of the deviation. The flat trend when  $\gamma = 0.2$  tells us that the time behavior of the dynamics is not sensitive to initial conditions. Thus, the case when  $\gamma = 0$  denotes the chaotic dynamics, whereas the case when  $\gamma = 0.2$  means no chaos.

The Lyapunov exponent (LE) is further discussed here. Figure 5(d) shows the results for the Lyapunov exponent as a function of  $A/\omega$ . Without system loss, the Lyapunov exponent is greater than zero, which implies that the dynamics is indeed chaotic. However, the almost flat curve when  $\gamma = 0.2$  reveals that the Lyapunov exponent is roughly equal to zero and such condition has no chaos.

According to the above discussion, we can conclude that localization can be significantly improved for weak loss and short evolution time. Within the parameter range of  $1 < A/\omega < 2$  and in the case of  $\gamma = 0$ , chaos can be observed and, with the assistance of chaos, atoms can tunnel into other sites. However, when  $\gamma = 0.2$ , the chaotic dynamics is destroyed and localization is enhanced. Thus, loss-induced localization in our proposal may originate from the destruction of chaotic dynamics due to system losses.

### B. Dependence of localization on nonlinearity

In the above discussion, nonlinearity is always fixed at  $U = 8$  and the dependence of system dynamics on nonlinearity is not clear. Here, we further discuss the influence of nonlinearity on loss-induced localization, and the results are plotted in Fig. 6. Since we mainly focus on the trend of change and considering the fragility of quantum states, the total integrating time is still chosen as 100 time units. In the case of  $A = 16$ ,  $\omega = 10$ ,  $\Omega = 1$ , Figs. 6(a) and 6(b) demonstrate the evolution of  $\min(P_1)$  with the increase of nonlinearity with two different system losses. When  $\gamma = 0$ ,  $\min(P_1)$  features a rich variety of effects related to the multiple transitions between tunneling and localization. However, in the case of  $\gamma = 0.2$ , there exists a nonlinear parameter window to observe localization within  $4 < U < 10$ . It is evident that the loss can be introduced to induce localization in an appropriate parameter range of nonlinearity.

Figures 6(c) and 6(d) correspond to the evolution of the Lyapunov exponent versus nonlinearity  $U$ , which further manifests the relationship between loss-induced localization and the disappearance of chaos. When  $\gamma = 0$ , the Lyapunov exponent in Fig. 6(c) is more than zero with the increase of nonlinearity, which implies that the dynamics are chaotic.

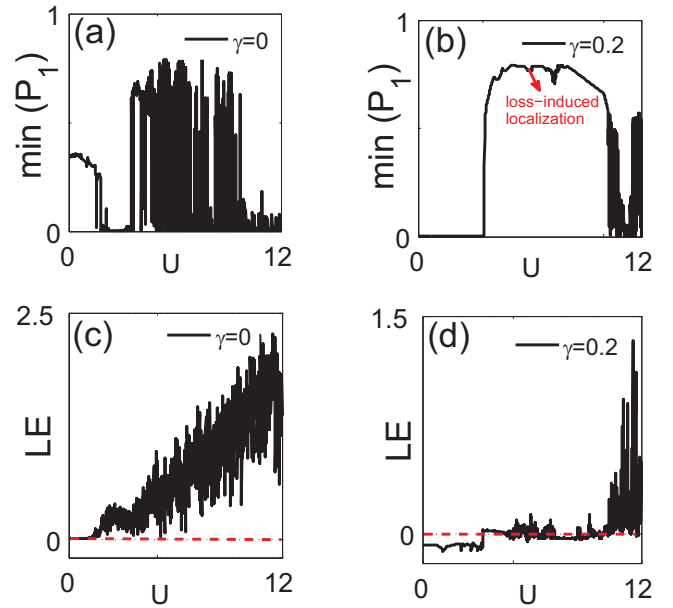


FIG. 6. (a), (b) The minimum value of  $P_1$  as a function of nonlinearity  $U$  for the two different conditions of  $\gamma = 0$  and  $\gamma = 0.2$ . (c), (d) Lyapunov exponent versus nonlinearity  $U$  when  $\gamma = 0$  and  $\gamma = 0.2$ . The horizontal dashed lines in panels (c) and (d) label the positions of  $\alpha = 0$ . Other parameters are  $A = 16$ ,  $\omega = 10$ ,  $\Omega = 1$ .

However, the Lyapunov exponent is less than or about equal to zero in Fig. 6(d) within  $4 < U < 10$ . Thus, it is the disappearance of chaos that induces the counterintuitive phenomenon of loss-induced localization.

### V. CONCLUSION

In conclusion, we present a comprehensive analysis of loss-induced localization in a nonlinear periodically driven three-site system. We have obtained a fascinating result of loss-induced localization which originates from the destruction of chaotic dynamics. When the loss  $\gamma$  is much smaller, the system dynamics exhibits chaotic motion and multiple transitions between chaos-related localization and tunneling are observed. Then the increased system losses could destroy the chaotic dynamics, resulting in loss-induced localization. However, the duration of localization is limited for a medial  $\gamma$ , and the leakage, possibly because of impedance matching between lattice points, occurs after a period of evolution time, which means no localization actually. The transient nature of localization can be understood analytically in the mean-field approximation. If a larger value of  $\gamma$  is extended, it is possible to find that localization is enhanced obviously. Even though we have not observed localization in an infinite evolution time, our results are meaningful in the control of quantum states. Thus, in our scheme, there are two types of localization, which originate from different physics, relying on whether chaotic behavior exists. Our proposal allows for the manipulation of quantum dynamics, such as going from tunneling to localization or from chaotic to nonchaotic regimes by adjusting the driving amplitude and frequency, system loss, or nonlinearity. Moreover, there exists a wide parameter window to observe loss-induced localization both

in the range of driving parameters and nonlinear parameters, which permits the experimental possibility with currently available technologies. Besides, our approach will expand the understanding of chaos-related localization and loss-induced localization and deepen the potential application of driven systems in quantum motors and quantum measurements.

## ACKNOWLEDGMENTS

The work was supported by National Key Research and Development Program of China (2016YFA0301203), Henan Provincial Department of Science and Technology Research Project (182102210405).

- 
- [1] G.-F. Wang, D.-F. Ye, L.-B. Fu, X.-Z. Chen, and J. Liu, *Phys. Rev. A* **74**, 033414 (2006).
- [2] B. Wu and Q. Niu, *Phys. Rev. A* **61**, 023402 (2000).
- [3] U. Peschel, T. Pertsch, and F. Lederer, *Opt. Lett.* **23**, 1701 (1998).
- [4] Y. Wu and R. Cote, *Phys. Rev. A* **65**, 053603 (2002).
- [5] Ch. Ding, J. Li, Zh. Zhan, and X. Yang, *Phys. Rev. A* **83**, 063834 (2011).
- [6] Ch. Ding, J. Li, X. Yang, D. Zhang, and H. Xiong, *Phys. Rev. A* **84**, 043840 (2011).
- [7] L. Li, X. Luo, X.-Y. Lü, X. Yang, and Y. Wu, *Phys. Rev. A* **91**, 063804 (2015).
- [8] G. Lu and W. Hai, *Phys. Rev. A* **83**, 053424 (2011).
- [9] S.-I. Chu and D. A. Telnov, *Phys. Rep.* **390**, 1 (2004).
- [10] S. Longhi, *Europhys. Lett.* **107**, 50003 (2014).
- [11] J. Gong, D. Poletti, and P. Hänggi, *Phys. Rev. A* **75**, 033602 (2007).
- [12] T. Salger, S. Kling, T. King, C. Geckeler, L. M. Molina, and M. Weitz, *Science* **326**, 1241 (2009).
- [13] F. Grossmann, T. Dittrich, P. Jung, and P. Hänggi, *Phys. Rev. Lett.* **67**, 516 (1991).
- [14] F. Grossmann, P. Jung, T. Dittrich, and P. Hänggi, *Z. Phys. B: Condens. Matter* **84**, 315 (1991).
- [15] H. Lignier, C. Sias, D. Ciampini, Y. Singh, A. Zenesini, O. Morsch, and E. Arimondo, *Phys. Rev. Lett.* **99**, 220403 (2007).
- [16] E. Kierig, U. Schnorrberger, A. Schietinger, J. Tomkovic, and M. K. Oberthaler, *Phys. Rev. Lett.* **100**, 190405 (2008).
- [17] X. Luo, L. Li, L. You, and B. Wu, *New J. Phys.* **16**, 013007 (2014).
- [18] P. W. Anderson, *Phys. Rev.* **109**, 1492 (1958).
- [19] L. Martin, G. Di Giuseppe, A. Perez-Leija, R. Keil, F. Dreisow, M. Heinrich, S. Nolte, A. Szameit, A. F. Abouraddy, D. N. Christodoulides, and B. E. A. Saleh, *Opt. Express* **19**, 13636 (2011).
- [20] L. Li, B. Wang, X.-Y. Lü, and Y. Wu, *Ann. Phys. (Berlin, Ger.)* **530**, 1700218 (2018).
- [21] X.-Y. Lü, H. Jing, J.-Y. Ma, and Y. Wu, *Phys. Rev. Lett.* **114**, 253601 (2015).
- [22] F. Kh. Abdullaev, Y. V. Kartashov, V. V. Konotop, and D. A. Zezyulin, *Phys. Rev. A* **83**, 041805(R) (2011).
- [23] A. Guo, G. J. Salamo, D. Duchesne, R. Morandotti, M. Volatier-Ravat, V. Aimez, G. A. Siviloglou, and D. N. Christodoulides, *Phys. Rev. Lett.* **103**, 093902 (2009).
- [24] O. Vazquez-Candanedo, J. C. Hernandez-Herrejon, F. M. Izrailev, and D. N. Christodoulides, *Phys. Rev. A* **89**, 013832 (2014).
- [25] D. M. Jović, C. Denz, and M. R. Belić, *Opt. Lett.* **37**, 4455 (2012).
- [26] X. Luo, J. Huang, and C. Lee, *Phys. Rev. A* **84**, 053847 (2011).
- [27] G. Lu, W. Hai, and Q. Xie, *Phys. Rev. A* **83**, 013407 (2011).
- [28] Th. Anker, M. Albiez, R. Gati, S. Hunsmann, B. Eiermann, A. Trombettoni, and M. K. Oberthaler, *Phys. Rev. Lett.* **94**, 020403 (2005).
- [29] A. Smerzi, S. Fantoni, S. Giovanazzi, and S. R. Shenoy, *Phys. Rev. Lett.* **79**, 4950 (1997).
- [30] S. Inouye, M. R. Andrews, J. Stenger, H.-J. Miesner, D. M. Stamper-Kurn, and W. Ketterle, *Nature (London)* **392**, 151 (1998).
- [31] Y. Wang, J. Gao, X.-L. Pang, Z.-Q. Jiao, H. Tang, Y. Chen, L.-F. Qiao, Z.-W. Gao, J.-P. Dou, A.-L. Yang, and X.-M. Jin, *Phys. Rev. Lett.* **122**, 013903 (2019).
- [32] A. Szameit, D. Blömer, J. Burghoff, T. Schreiber, T. Pertsch, S. Nolte, A. Tünnermann, and F. Lederer, *Opt. Express* **13**, 10552 (2005).
- [33] A. Szameit, J. Burghoff, T. Pertsch, S. Nolte, A. Tünnermann, and F. Lederer, *Opt. Express* **14**, 6055 (2006).
- [34] I. L. Garanovich, S. Longhi, A. A. Sukhorukov, and Y. S. Kivshar, *Phys. Rep.* **518**, 1 (2012).
- [35] S. Longhi, *Laser Photonics Rev.* **3**, 243 (2009).
- [36] D. N. Christodoulides, F. Lederer, and Y. Silberberg, *Nature (London)* **424**, 817 (2003).
- [37] R. El-Ganainy, D. N. Christodoulides, C. E. Rueter, and D. Kip, *Opt. Lett.* **36**, 1464 (2011).
- [38] N. K. Efremidis, P. Zhang, Z. Chen, D. N. Christodoulides, C. E. Rueter, and D. Kip, *Phys. Rev. A* **81**, 053817 (2010).
- [39] M. Holthaus, *Phys. Rev. A* **64**, 011601(R) (2001).
- [40] D. A. Zezyulin, V. V. Konotop, G. Barontini, and H. Ott, *Phys. Rev. Lett.* **109**, 020405 (2012).